

ANN-Driven Adaptive Power Allocation for OWC

Walter Zibusiso Ncube, Ahmad Adnan Qidan, Taisir El-Gorashi and Jaafar M. H. Elmirghani

Abstract—Vertical-cavity surface-emitting lasers (VCSELs) have gained popularity in Optical Wireless Communication (OWC) due to their high bandwidth and directional beam compared to Light-emitting diodes (LEDs). In this work, we explore the deployment of VCSELs as Access Points (APs) in an indoor environment with time-varying user distributions and traffic demands. To enhance performance, a merged access point (MAP) topology is introduced to extend the serving area of each cell using Zero Forcing (ZF) for interference management. A power allocation optimisation problem is formulated aimed at maximising the sum rate of the dynamic network. Deterministic approaches can solve the formulated problem but are impractical for real-time scenarios. In this work, we propose an Artificial Neural Network (ANN) for adaptive power allocation with reduced computational complexity. Our results show that the designed ANN learns and effectively provides instantaneous solutions in dynamic scenarios, resulting in improved performance in terms of sum rate compared to a baseline uniform power allocation scheme.

Index Terms—Optical Wireless Communication Networks, Next Generation Communication Networks, VCSELs, Power Allocation, Machine Learning, Artificial Neural Networks

I. INTRODUCTION

OWC has emerged as an enabler for next-generation networks, offering unregulated bandwidth for better performance. Early OWC systems using LEDs were constrained by bandwidth. However, advancements have introduced laser-based OWC systems, particularly VCSELs, which deliver focused beams for efficient power use, higher data rates, and longer transmission distances [1]. Despite these advantages, numerous VCSEL deployment is required to ensure spatial coverage resulting in inter-cell interference, which can be lessened by merging optical APs into larger cells to enhance coverage [2]. However, these larger cells demand efficient power use to maintain a balance between performance and sustainability.

In general, efficient resource management is crucial for maximising network performance. Optimisation problems aimed at rate maximisation have been extensively investigated to enhance the efficiency of OWC networks. In [3] and [4] resource allocation strategies were explored to optimise system performance. However, such methods are inherently complex and computationally intensive with increasing network size, posing significant challenges for real-time implementation.

To address these limitations, Machine Learning (ML) has emerged as a promising solution for NP-hard optimisation problems [5]–[7]. In [5], a deep learning algorithm was employed for resource allocation in massive MIMO systems, achieving high performance with minimal computational overhead. Similarly, [6] introduced an ANN model in a laser-based OWC network that allocated fractional time resources based on traffic demands with low computational overhead

in real-time. Furthermore, in [7] cooperative ANNs were designed for sum rate maximisation in a discrete-time laser-based OWC system delivering a near-optimal solution. Despite these advancements, the application of ML in OWC networks remains an evolving field, particularly for dynamic, real-time scenarios.

In this paper, we train an ANN to solve a power allocation optimisation problem that aims to maximise the sum rate in two different OWC network topologies. The optimisation problem is split into two subproblems: a user association subproblem and a power allocation subproblem. The user association sub-problem is solved using a low-complexity algorithm and an ANN model is designed and trained to deliver fast and real-time power allocation.

II. SYSTEM MODEL

We consider an indoor laser-based OWC network designed to deliver high data rate communication. $A, a = \{1, \dots, A\}$, optical APs are located on the ceiling where each optical AP is designed as a micro lens VCSEL array for data transmission. The APs are arranged into $C, c = \{1, \dots, C\}$, multiple optical cells and serve $U, u = \{1, \dots, U\}$, users on the communication plane with time-varying distribution and traffic demands. We define the set of users within the coverage area of cell c as $U_c, u = \{1, \dots, U_c\}$. Users are equipped with a multi-photodiode optical detector for better field of view (FoV) and signal reception.

All the optical APs with a WiFi AP for uplink transmission are connected to a centralized unit (CU), which provides AP-coordination and resource management. The system supports two distinct cell configurations: the Traditional cell formation and the Merged Access Point cell formation. In the traditional system, each AP independently defines a discrete optical cell. While this design is simple and effective for small setups, it has challenges in larger networks due to ICI from overlapping Line-of-sight (LoS) beams as shown in Fig. 1 (left). Note that, narrowing the receiver’s FoV can reduce ICI but leads to coverage gaps and frequent handovers, causing performance degradation, i.e., low quality of service (QoS) [8]. To address this, we introduce the Merged Access Point (MAP) configuration as in our previous work [9], which combines adjacent APs into a larger optical cell as depicted in Fig. 1 (right). The system uses Zero-Forcing (ZF) for interference management, ensuring seamless coverage and improved user experience [9], [8]. For more information, we refer readers to [9].

A. Transmit optical power

We assume that the VCSEL beam exhibits a Gaussian profile which is characterized by two key parameters: the



Fig. 1. Traditional (left) and MAP (right) cell formations.

beam waist (w) and the wavelength (λ). For a Gaussian beam propagating along the z -axis, the intensity distribution is given by:

$$I(r, z) = \frac{2P_t}{\pi w^2(z)} \exp\left(-\frac{2r^2}{w^2(z)}\right), \quad (1)$$

where P_t is the transmitted optical power, r and z represent the radial and axial positions, respectively, and $w(z)$ is the beam spot radius as a function of z . In this study, we consider the parameters of the Gaussian beam after being refracted through a lens as in [9]. The total transmitted power from an $n \times n$ VCSEL array is the cumulative output power of all individual VCSELs of the array, $P^a = \sum_{i=1}^{n \times n} P_t^i$, where P_t^i represents the transmitted power of the i -th VCSEL. To ensure compliance with eye safety standards, the total emitted power from an AP or array must not exceed the permissible limits, P_{safe} , such that $P^a \leq P_{\text{safe}}$ [9].

III. SUM DATA RATE OPTIMISATION PROBLEM

We first define the achievable data rate of user u assigned to cell c^1 regardless of the cell configuration as follows:

$$R_u^c = B_0 \log_2 \left(1 + \left(\frac{e}{2\pi} (\gamma_u^c)^2 \right) \right), \quad (2)$$

where B , is the bandwidth, e is Euler's number and γ_u^c is:

$$\gamma_u^c = \frac{E \left[(P_u^c)^2 \right]}{|\mathbf{L}\mathbf{H}\mathbf{H}^{\mathbf{H}}|^2 \cdot E \left[|\sigma_n^2|^2 \right]}, \quad (3)$$

P_u^c is the allocated power of user u from cell c . The variance σ_n^2 is given by $N_u^d B$ where N_u^d is noise power spectral density, considered per cell and calculated as in our previous work [10].

We now formulate an optimisation problem based on maximising the system sum rate as follows:

¹For clarity, a cell c is one AP for the traditional cell configuration, and can be at least two APs for the MAP configuration.

$$\max \sum_{u \in U} \sum_{c \in C} \log(S_u^c R_u^c) \quad (4)$$

subject to:

$$\sum_{c=1}^C S_u^c = 1, \quad \forall u \in U, \quad (5)$$

$$P_u^{\min} \leq \sum_{c=1}^C S_u^c P_u^c \leq P_u^{\max}, \quad \forall u \in U, \quad (6)$$

$$\sum_{u=1}^{U_c} P_u^c \leq P^c \quad \forall u \in U_c, \quad (7)$$

where S_u^c is a binary assignment term that denotes whether or not user u is assigned to cell c . Constraint (5) ensures that each user is assigned to exactly one cell. Constraint (6) ensures that the minimum demand for each user is met and if the cell is not overloaded, more power is allocated to the user until it reaches the maximum power permissible for the user. Constraint (7) is a capacity constraint that ensures that the total power assigned to all the users U_c within the coverage area of the cell does not exceed the cell's capacity. Note that, $P^c = P^a$ for the traditional cell configuration, and $P^c = \sum_{a \in A_c} P^a$ for the MAP cell configuration where A_c is the number of APs belonging to cell c . The optimisation problem in (4) is NP-hard due to the coupling of S_u^c and P_u^c , and it has complexity of $\mathcal{O}(C^U)$. Therefore, and we decompose it into two subproblems: a user association subproblem and a power allocation subproblem and we solve these using efficient algorithms. The user association subproblem is given by:

$$\max \sum_{u \in U} \sum_{c \in C} \log(S_u^c R_u'^c), \quad (8)$$

where $R_u'^c$ is the data rate under fixed power allocation. (8) can be solved subject to constraint (5) using predefined signal strength threshold-based search or heuristic algorithm, as in [11], which has low-complexity of $\mathcal{O}(U \times C_{th})$, $C_{th} < C$.

The user association vector is input into the power allocation subproblem which is solved using an ANN trained to optimise the power allocation vector. We solve the two subproblems iteratively, and in each iteration, the user association vector and the power allocation vector are alternately updated. This process continues until convergence is achieved, and sub-optimal solutions for the original optimisation problem is obtained.

IV. POWER ALLOCATION ARTIFICIAL NEURAL NETWORK

We use a Convolution Neural Network (CNN), which is one of the common ANNs known for its efficiency and speed. In this work, the input layer of the CNN corresponds to information from the system such as the user association vector and QoS demands. Moreover, the hidden layer has B hidden layers and each layer has a total of A artificial neurons. We determine the output of each neuron, $z_{a,b}$, as follows [6]:

$$z_{a,b} = \alpha_{a,b} [\mathbf{w}_{a,b} \otimes z_{o,b-1} + \zeta_{a,b}], \quad (9)$$

where $\alpha[\cdot]$ is an activation function, $\mathbf{w}_{a,b}$ is the weight vector of the a -th neuron in the b -th layer, \otimes is the convolution operator of the CNN, $z_{o,b-1}$ is the output of layer $b-1$ and $\zeta_{a,b}$ is a scalar bias. Finally, the output layer determines the power allocated to each user and the available power budget of each optical cell.

A. Dataset Generation

We aim to train the ANN so that it establishes a mapping function $f(M; \cdot)$ that allocates power based on user association, user demands, and other system constraints as in the optimisation problem. Lets assume M as a set of weight terms that serve as a bridge between the input and output layers. In this context, we must generate a dataset for training the ANN to select the optimal set of parameters, M^* , that provides the maximisation of the system's sum rate in real-time scenarios.

We generate a dataset comprising N data points. Each data point n corresponds to the user association and user requirements within the range $P_u^{\min} \leq P_u \leq P_u^{\max}$ to C cells. The power allocated to a specific user varies for each user based on their serving cells, and their activity at a given time, i.e., $P_u \neq P_{u'}$ for $u \neq u'$.

The dataset must also account for maximising the sum rate of the users. Therefore, after solving (8), each cell c independently maximizes the sum rate of its own users as follows

$$\begin{aligned} \max_{P_u^c} & \left[\sum_{u \in U_c} \log(R_u^c) - \omega_c \left(\sum_{u \in U_c} P_u^c - P^c \right) \right. \\ & \left. - \sum_{u \in U_c} \beta_{u,1} \left(P_u^c - P_u^{\max} \right) + \sum_{u \in U_c} \beta_{u,2} \left(P_u^{\min} - P_u^c \right) \right], \end{aligned} \quad (10)$$

where ω_c , β_1 , and β_2 are multipliers corresponding to the cell capacity and user requirement constraints. To solve this problem, the optimal power allocated to each user by a cell is determined using the Karush-Kuhn-Tucker (KKT) conditions [12]. An iterative process is then applied to update the multipliers using gradient-based algorithms as follows:

$$\begin{aligned} \omega_c^{(i+1)} &= \left[\omega_c^{(i)} - \varphi_{\omega}^{(i)} \left(\sum_{u \in U} P_u^{c*} - P^c \right) \right]^+, \\ \beta_{u,1}^{(i+1)} &= \left[\beta_{u,1}^{(i)} - \varphi_{\beta_1}^{(i)} \left(P_u^{c*} - P_u^{\max} \right) \right]^+, \\ \beta_{u,2}^{(i+1)} &= \left[\beta_{u,2}^{(i)} - \varphi_{\beta_2}^{(i)} \left(P_u^{\min} - P_u^{c*} \right) \right]^+, \end{aligned} \quad (11)$$

where $[\cdot]^+$ represents a projection onto the positive orthant to ensure $\omega_c, \beta_{u,1}, \beta_{u,2} \geq 0$, $\varphi_j^{(i)}$ ($j \in \{\omega_c, \beta_1, \beta_2\}$) is the step size at iteration i , P_u^{c*} is the optimal power allocation for user u from cell c . After solving the optimisation problem for various user distributions and activities, the maximized rates are recorded to create a training dataset for the ANN model.

B. ANN Implementation

1) *Offline Phase*: In training of the ANN model, our aim is to identify the optimal set of weight terms, M^* , that aligns the

TABLE I
SYSTEM PARAMETERS

| Description | Value | Description | Value |
|----------------------------|-----------------|----------------------------|------------|
| Beam waist radius | 5 μm | VCSEL wavelength | 1050 nm |
| RIN Power Spectral Density | -155 dB/Hz | Lens refractive index | 1.55 |
| Receiver refractive index | 1.77 | Photodetector responsivity | 0.7 A/W |
| ADR half-angle FOV | 30° | Preamplifier noise figure | 5 dB |
| System bandwidth | 3.5 GHz | Validation dataset size | 10% of N |
| ANN hidden layers | 3 | Training dataset size | 90% of N |

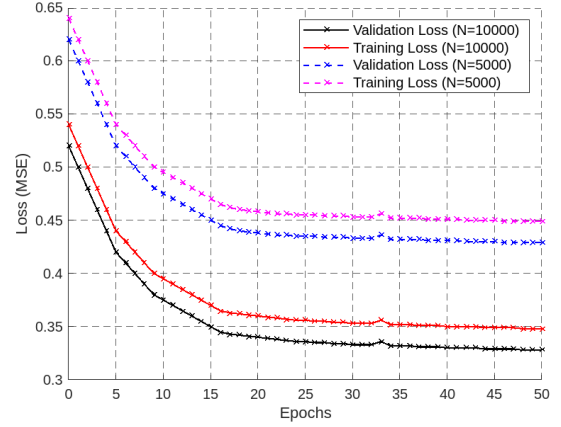


Fig. 2. Training and validation for two different dataset sizes.

ANN model's input and output. The training dataset consists of N data points, where the n -th data point is represented by the input $\mathbf{v}(n)$ and the corresponding optimal power allocation $\mathbf{P}^*(n)$. The output layer of the ANN estimates the power allocation vector $\hat{\mathbf{P}}(n)$. The ANN model learns by minimising a loss function between the estimated power allocation and the optimal allocation, i.e., $\min \frac{1}{N} \sum_{n=1}^N \Theta(\hat{\mathbf{P}}(n), \mathbf{P}^*(n))$, where $\Theta(\cdot, \cdot)$ denotes the mean-square-error (MSE) function. In this way the ANN can be trained to provide sub-optimal solutions in time-varying scenarios, including those not explicitly covered in the training dataset.

2) *Real-Time Phase*: After training, the ANN is deployed to perform power allocation in real time. In this phase, the model determines the power allocation for users based on their locations and requirements, available resources of the cells, and system constraints. Cells and users iteratively update their multipliers, $\omega_c, \beta_{u,1}$ and $\beta_{u,2}$, based on the output of the ANN model. These updates follow gradient-based methods to ensure that power allocation satisfies the constraints and maximises efficiency. Additionally, the ANN dynamically updates power allocation everytime user requirements and distributions change.

V. RESULTS AND DISCUSSION

We consider a 5 m \times 5 m \times 3 m indoor environment with 16 APs uniformly distributed across the ceiling to serve 8 users on the communication plane at a distance of 2 m from the ceiling. We model user mobility using the Random Waypoint model where each user moves between randomly selected waypoints with speed ν as in [13]. Moreover, the arrival of user requests is represented by a Poisson process with arrival rate μ , and the duration of these demands follows a hyper-exponential

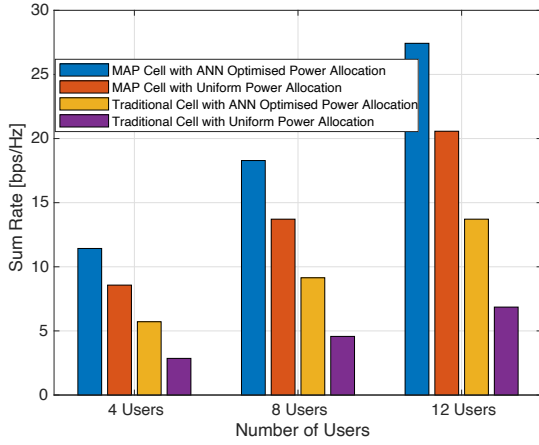


Fig. 3. Sum rates of different cell schemes. $\gamma = 20dB$, $N = 10000$.

distribution to account for variability in user behavior as in [14]. Other simulation parameters are in Table 1.

The training and validation loss curves in Fig. 2 indicate that the ANN is effectively learning from the data. For both dataset sizes ($N = 5000$ and $N = 10000$), the training loss decreases steadily over epochs, demonstrating that the performance of the model improves in the training data. Similarly, the validation loss decreases with the time, indicating that the model generalizes well to the validation data. Furthermore, the ANN model for both dataset sizes avoids over-fitting and delivers acceptable solutions validating its ability to provide solutions in dynamic real-time scenarios. Also, our results show the positive impact of using a larger dataset, which was effectively used.

Without loss of generality, we consider a 4-AP MAP cell as shown in Figs. 3 and 4, other cell sizes can be considered. Our results show that the MAP cell configuration outperforms the traditional scheme in terms of sum rate. This is due to the enhanced signal coverage and power provided by the additional APs operating together. However, ZF may become less effective for managing transmissions as the number of users belonging to a cell increases. The results also show that the ANN-optimised power allocation scheme outperforms the uniform power allocation scheme at different SNRs and numbers of users. The ANN-optimised scheme dynamically adapts to any updates in the network, unlike the uniform approach, which allocates the same power to all users regardless of their conditions.

CONCLUSION

In this study, we formulated an optimisation problem for rate maximisation in a laser-based OWC system considering two different AP cell formation schemes. We designed an ANN that allocates power to mobile users with varying demands in an indoor environment. Our findings reveal that the ANN-optimised power allocation scheme outperforms the uniform power allocation scheme by dynamically adjusting power allocation to meet user demand and distribution. Also, the results indicate that the MAP cell formation achieves better performance than the traditional cell design. This enhanced

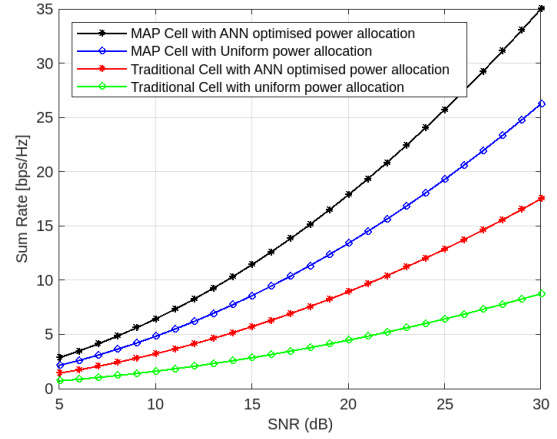


Fig. 4. Sum rates vs SNR. $U = 8$, $N = 10000$.

performance is due to the improved signal coverage where multiple APs operate collaboratively. However, increasing cell size introduces added complexity in network management and requires more advanced interference management strategies.

REFERENCES

- [1] E. Sarbazi, H. Kazemi, M. Dehghani Soltani, M. Safari, and H. Haas, "A tb/s indoor optical wireless access system using vcsel arrays," in *2020 IEEE 31st Annual International Symposium on Personal, Indoor and Mobile Radio Communications*, 2020, pp. 1–6.
- [2] R. Zhang, H. Claussen, H. Haas, and L. Hanzo, "Energy efficient visible light communications relying on amorphous cells," *IEEE Journal on Selected Areas in Communications*, vol. 34, no. 4, pp. 894–906, 2016.
- [3] M. S. Uddin, M. Z. Chowdhury, and Y. M. Jang, "Priority-based resource allocation scheme for visible light communication," in *2010 Second International Conference on Ubiquitous and Future Networks (ICUFN)*, 2010, pp. 247–250.
- [4] M. Ju, X. Li, Y. Gan, Y. Li, G. Tan, and P. Huang, "Resource allocation in underwater wireless optical communication systems," in *2022 IEEE 22nd International Conference on Communication Technology (ICCT)*, Nov 2022, pp. 357–362.
- [5] L. Sanguinetti, A. Zappone, and m. Debbah, "Deep learning power allocation in massive mimo," 10 2018, pp. 1257–1261.
- [6] A. A. Qidan, T. El-Gorashi, and J. M. H. Elmirghani, "Artificial neural network for resource allocation in laser-based optical wireless networks," in *ICC 2022 - IEEE International Conference on Communications*, 2022, pp. 3009–3015.
- [7] —, "Cooperative artificial neural networks for rate-maximization in optical wireless networks," in *ICC 2023 - IEEE International Conference on Communications*, 2023, pp. 1143–1148.
- [8] X. Li, R. Zhang, J. Wang, and L. Hanzo, "Cell-centric and user-centric multi-user scheduling in visible light communication aided networks," in *2015 IEEE International Conference on Communications (ICC)*, 2015, pp. 5120–5125.
- [9] W. Z. Ncube, A. A. Qidan, T. El-Gorashi, and J. M. H. Elmirghani, "Optimised energy efficiency of various cell sizes in laser-based optical wireless communications," in *MeditCom*, 2024, pp. 389–394.
- [10] W. Z. Ncube, A. A. Qidan, T. El-Gorashi, and M. H. Jaafar Elmirghani, "On the energy efficiency of laser-based optical wireless networks," in *NetSoft*, 2022, pp. 7–12.
- [11] X. Wu, M. Safari, and H. Haas, "Access point selection for hybrid li-fi and wi-fi networks," *IEEE Transactions on Communications*, vol. 65, no. 12, pp. 5375–5385, 2017.
- [12] D. Bertsekas, *Nonlinear Programming*, 2nd ed. Athena Scientific, 2003.
- [13] M. Dehghani Soltani, A. A. Purwita, Z. Zeng, C. Chen, H. Haas, and M. Safari, "An orientation-based random waypoint model for user mobility in wireless networks," in *ICC Workshops*, 2020, pp. 1–6.
- [14] M. Ismail and W. Zhuang, "Decentralized radio resource allocation for single-network and multi-homing services in cooperative heterogeneous wireless access medium," *IEEE Transactions on Wireless Communications*, vol. 11, no. 11, pp. 4085–4095, 2012.